International Journal of Pharmaceutics 432 (2012) 23–31

Contents lists available at SciVerse ScienceDirect

International Journal of Pharmaceutics

journal homepage: www.elsevier.com/locate/ijpharm

# Effect of expansion chamber geometry on atomization and spray dispersion characters of a flashing mixture containing inerts. Part I. Numerical predictions and dual laser measurements

Dehao Ju[a], John Shrimpton[a,*], Moira Bowdrey[b], Alex Hearn[b]

[a] Energy Technology Group, School of Engineering Sciences, Highfield Campus, University of Southampton, Southampton SO17 1BJ, UK
[b] Kind Consumer Limited, London, UK

ARTICLE INFO

*Article history:*
Received 28 October 2011
Received in revised form 22 April 2012
Accepted 23 April 2012
Available online 28 April 2012

*Keywords:*
Nicotine
Smoking
Metered dose inhalers
Breath activation

ABSTRACT

A cigarette alternative is designed to deliver a dose of medicinal nicotine within a timeframe comparable to that of a cigarette, and gives much of what smokers expect from a cigarette without the risks of smoking tobacco. The design concept is the same as a pressurized metered dose inhaler (pMDI), but is a breath actuated device (Oxette®). This work predicts the residual mass median diameter (MMD) of the spray issuing from early stage Oxette® prototypes by using an evaporation model of multi-component liquid droplets with the help of a numerical multi-component two-phase actuation model (developed by the authors) to quantify the sprays. Two different formulations with 95% and 98% mass fraction of HFA 134a, and two prototypes of cigarette alternatives with different expansion chamber volumes have been analyzed by the numerical model and compared with laser based measurements. The later designed device provides a larger expansion chamber volume to enhance the propellant evaporation, recirculation, bubble generation and growth inside the chamber, and it makes a significant improvement to produce finer sprays than the earlier design. The mass fraction of the formulation does not affect significantly on the initial MMD of the droplets near the discharge orifice. However, it influences the residual MMD at $x = 100$ mm from the discharge orifice, where the ratio of the predicted residual MMDs of the droplets generated by the formulations with 98% and 95% of HFA 134a is 0.73. Although the formulation with 98% of HFA 134a can generate smaller droplets, the formulation with 95% of HFA 134a produces more steady puffs with relatively low mass flow rate.



## 1. Introduction

Tobacco smoking is a health epidemic of almost unparalleled proportions. The World Health Organization believes, if current trends continue, tobacco-related illnesses can be responsible for up to one billion premature deaths in the 21st century (Scollo et al., 2003). Kind Consumer Ltd. believes innovation into practical alternatives for the tobacco user is the key in saving lives. If an effective, affordable and safe replacement for the tobacco cigarette can be adopted widely by smokers who cannot or will not quit, it would deliver far-reaching public health benefits by saving thousands of life years lost prematurely in every generation. There is an emerging consensus supported by a wealth of science, that pure medicinal nicotine is a 'very safe drug' (Medicines Healthcare Products Regulatory Agency, 2010). It is the combustion of the tobacco and the toxic nature of the smoke generated that causes harm, not the nicotine itself. Kind Consumer Ltd. has developed technology designed as a breakthrough innovation which aims to be the first medically approved and regulated cigarette alternative. It is designed to deliver a dose of medicinal nicotine within a timeframe comparable to that of a cigarette, and gives much of what smokers expect from a cigarette without the risks of smoking tobacco. The technology is a non-electronic, pressure-driven nicotine delivery system that delivers a reproducible dose of formulation targeted for lung delivery as an aerosol released from the device via a breath-operated valve. The technology contains no tobacco and does not involve combustion or heat of any nature in its operation. A user actuates the valve to regulate their nicotine intake in a manner similar to that of smoking.

The working principle of the cigarette alternative is similar to pressurized-metered dose inhalers (pMDIs). Through breath-actuation, the formulation flows through a twin-orifice domain to form an aerosol by flashing atomization. The simplified actuation flow domain has been illustrated by Ju et al. (2010).

The expansion chamber, upstream of the atomizer discharge orifice, is a key component to producing fine sprays from pMDI

* Corresponding author.
*E-mail address:* John.Shrimpton@soton.ac.uk (J. Shrimpton).

0378-5173/$ – see front matter © 2012 Elsevier B.V. All rights reserved.
http://dx.doi.org/10.1016/j.ijpharm.2012.04.065

like devices. Gebauer (1901, 1902) concluded that a spray can be produced only when the inlet orifice diameter ($d_i$) is smaller than the discharge orifice diameter ($d_e$). When the ratio was larger than unity, a jet is generated. Rotheim and Fulton (1933, 1950 as cited in Sanders, 1970) found that the finest spray is acquired when the $d_i$ is 0.38 mm and the $d_e$ is 0.53 mm ($d_i/d_e = 0.72$). Katz-Zeigerson and Sher (1998) found that, with injection conditions in the pressure range of 200–600 kPa and temperature range of 25–60 °C, the optimal ratio ($d_i/d_e$) is between 0.6 and 0.75. With large orifice diameter ratios ($d_i/d_e > 2$), no bubbles were observed. For ratios between 1.1 and 1.8, a stratified oscillating flow occurs, supplemented with bubble coalescence, while with orifice diameter ratios between 0.65 and 0.8, a homogeneous bubbly flow prevails throughout the whole chamber volume.

Rashkovan and Sher (2006) analyzed how the length of the expansion chamber affects the flow, where the orifice diameter ratio is 0.68 and the chamber diameter ($D_{CH}$) is 10 mm during the experiment. When a chamber length of 5 mm is used, the liquid flows straight through the chamber and through the discharge orifice without impinging on the opposite chamber wall. It has been observed that for a longer chamber (10 mm, 30 mm and 50 mm), a notable backflow occurs along the walls of the chamber, which indicates a toroidal vortex flow inside the chamber. The backflow along the chamber walls diminishes for long chambers and/or high orifice diameter ratios. At the center of the 10 mm long chamber, non-homogeneous regions were found. The large gas bubbles develop in the vortex core and, after reaching an appreciable size, are expelled outward toward the chamber wall. This expelling process leads to periodic short non-uniformities in the spray. A further increase of the length of the chamber to 30 mm causes toroidal vortex stretching and decreases rotation speed and, consequently, the non-uniformities in the flow pattern disappear. A homogeneous bubbly flow prevails throughout the whole volume of the chamber. For a chamber of 50 mm, a similar flow pattern to that shown for the 30 mm long chamber occurs. In this case, however, a longer residence time for the bubbles is available; consequently, the bubbles are larger, the larger bubbles experience greater buoyancy and flow stratification develops: a bubbly flow in the upper part of the chamber and a liquid flow in the lower part.

The direct objectives of the current work were to study how expansion chamber volumes and different formulations affect the flashing atomization, with a view to supporting the development of the cigarette-like, breath activated pMDI atomizer (named here as Oxette®). A mathematical model (Ju et al., 2010) is implemented to investigate the multi-component two-phase flow characteristics of flashing flow, with the aim of optimizing the process to provide very fine atomization, and to evaluate the effect of different formulations on the spray characteristics for different expansion chamber geometry.

Here, a mechanical lung has been designed to actuate the Oxette® under different smoking profiles (Tobin et al., 1982). Spray velocities and duration were measured using the dual laser method (Ju et al., 2010). Measurements were performed using HFA-propelled formulation within an Oxette®, and the analysis in performance with different steps of actuations as well as for different formulations (especially with different propellant mass fraction) actuated under different smoking profiles was undertaken.

This work will be useful for future researchers investigating flash evaporation systems since it informs on the effect of both geometrical and formulation changes, including presence of inerts (non-volatile components) on the final spray quality, and provides verification of a model used to predict such changes.

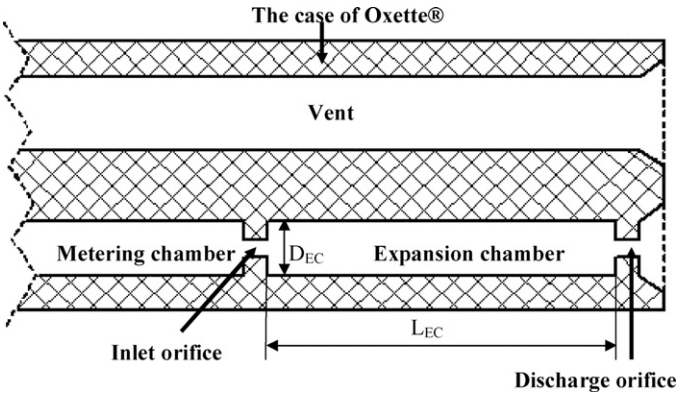


**Fig. 1.** Schematic diagram of Oxette® ($D_{EC}$: expansion chamber diameter, $L_{EC}$: expansion chamber lengths). The formulation residing in the metering chamber is actuated through the expansion chamber to from a spray via the discharge orifice.

## 2. Method

### 2.1. Experimental measurement method

Two prototypes with different expansion chamber lengths were provided by Kind Consumer Ltd. for analysis, named here as Oxette® 1 for the earlier design and Oxette® 2 for the later design. A schematic diagram of the Oxette® is shown in Fig. 1. The same dimensions of the two devices are the metering chamber volume of 600 $mm^3$, the discharge orifice diameter ($d_e$) of 0.2 mm and the expansion chamber diameter ($D_{EC}$) of 1.0 mm. The inlet orifice diameters ($d_i$) change between 0.14 mm and 0.18 mm due to the inhaled pressure variation, and a mean value of 0.17 mm is used in the simulation. The expansion chamber lengths ($L_{EC}$) of Oxette® 1 and Oxette® 2 are 2.0 mm and 6.9 mm respectively. The formulation is actuated from the metering chamber, and flows through the expansion chamber to the ambient via the discharge orifice. The vent is open to the atmosphere.

In order to test the mechanical operation and measure the performance characteristics of a breath actuated Oxette®, a test rig to simulate the effect of human inhalation has been designed. Since there is a broad spectrum of human respiratory behaviour, due to factors such as aging, health and medical conditions such as asthma, an important requirement for the test apparatus is that it is flexible enough to accurately reproduce a range of human inhalation responses. With this in mind, the test device has been designed on the basis of reproducibility and controllability. This has been achieved by basing the rig around a computer controlled electromechanical setup, commonly used in high-precision automation applications. The rig design primarily consists of a mechanically driven piston-cylinder arrangement simulating diaphragm motion to model the changes in human lung volume during inhalation. This is coupled to a transparent inspection chamber to facilitate visual inspection and optically based measurements of the aerosolized product to be tested.

The shallow and deep smoking profiles have been programmed to control the piston movement, referring to the lung volume variations of different smokers from the experimental work by Tobin et al. (1982). Pressure variations in the lung under two smoking patterns detected by the pressure sensor installed in the mechanical lung were recorded as shown in Fig. 2, where $p_{inhalation}$ is the inhalation pressure and $p_{atm}$ is atmospheric pressure.

In order to verify the numerical model, and acquire the key information on the actuation simply and reliably, the dual laser beam method (Ju et al., 2010) is applied to measure the spray velocity, duration and relative opacity at two positions of $x = 25$ mm and $x = 100$ mm from the discharge orifice. The former station

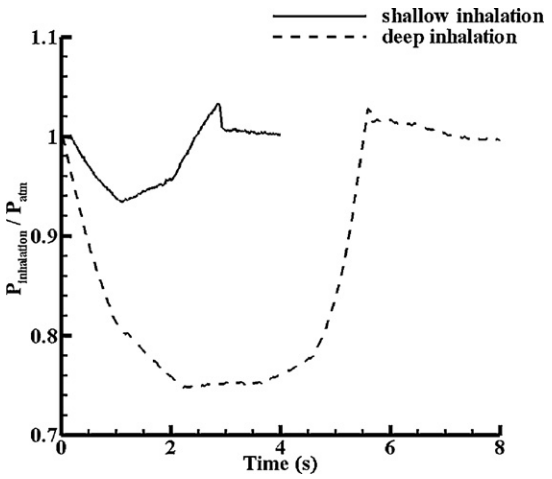


**Fig. 2.** Pressure variations in the "lung" under shallow and deep smoking profiles (Tobin et al., 1982), measured by the pressure senor installed in the mechanical lung ($p_{inhalation}$: inhalation pressure, $p_{atm}$: atmospheric pressure).

represents the location close to the discharge orifice and latter one is at an approximate distance from the discharge orifice to the human oropharynx (Placke et al., 2006).

### 2.2. Mathematical modeling of a pMDI

A multiphase, multi-component transient model of the key components of a typical metered dose inhaler has been developed and experimentally verified using the dual beam method and a range of propellant formulations (Ju et al., 2010). This model is implemented to simulate the actuation flow issuing from two prototypes (Oxette® 1 and Oxette® 2) introduced in Section 2.1.

The objective of the design of the Oxette® is to acquire steady, relatively slow spray which should be fine enough to be inhaled deeply into the lung and to have the appearance of cigarette smoke. During a single inhalation, the mass flow rate of the nicotine is required to be relatively constant. The formulations with different mass fraction of propellant HFA 134a produce the sprays with different quality, exit velocity and duration. Five different nicotine formulations have been tested using pMDI in our previous work (Ju et al., 2010), and the formulation with mass fraction of HFA 134a above 80% was recommended. Therefore another two different formulations with high mass fraction of HFA 134a were tested in this work, and they are named here as Formulation 1 with 95% mass fraction of propellant and Formulation 2 with 98% mass fraction of propellant. The physical properties of the propellant each component are listed in the previous publication (Ju et al., 2010). The remaining components are non-volatile and inert.

From the experiment by Clark (1991), initial mass median diameter (MMD) of the spray generated at the discharge orifice from a typical pMDI may be estimated from the quality of the fluid ($q_{ec}$: gas/total fluid mass ratio) and the pressure ($P_{ec}$) in the expansion chamber by Eq. (1). This has been implemented in the multiphase, multi-component transient model (Ju et al., 2010) to give a further indicator of spray quality.

$$\mathrm{MMD} = \frac{8.02}{q_{ec}^{0.56}((p_{ec} - p_{atm})/p_{atm})^{0.46}} \quad (1)$$

In reality, we are only interested in the droplet sizes at the axial position from the discharge orifice of $x = 100$ mm where the human oropharynx locates and it provides important information on the droplet depositions in the human respiratory tract in order to predict the efficacy of the formulation. Generally it is a combination of evaporation and boiling processes after the liquid discharging from the discharge orifice (Polanco et al., 2010). Brenn et al. (2007) developed an evaporation model of multi-component liquid droplets. The liquid phase is treated as a thermodynamically real fluid, using the Universal Functional Activity Coefficient (UNIFAC) method for calculating the component activities, and the gas phase as ideal. The properties of structure groups in different molecules of the propellant and inerts can be referred to Reid et al. (1977), Fukuchi et al. (2001), Wittig et al. (2003) and Hou et al. (2008).

Some assumptions are required to predict residual droplet sizes at $x = 100$ mm:

1. The flow discharged from the Oxette® is an axisymmetrically turbulent jet with a constant spreading rate (Pope, 2000), and the cone angle of the spray was formed to be, 21.6° which was also measured by Dunbar (1996) for a pMDI device.
2. Fig. 3 indicates the control volume (CV) is assumed to be a trapezoid and its volume per time interval can be calculated by the cone angle and the local mean velocities ($\bar{u}_1$ in $CV_1$ and $\bar{u}_2$ in $CV_2$). At the beginning of the actuation at the orifice exit, it is assumed the control volume is full of liquid.
3. The initial conditions of the droplets at the exit of the discharge nozzle, such as droplet velocity and temperature, are predicted by the multi-component two-phase flow model (Ju et al., 2010).
4. All the droplets are assumed to be spherical and same size and uniformly distributed in the control volume along the jet, traveling with the same velocity. The initial mass fraction of each component in the droplets is the same as that of the original formulation.
5. The flow is actuated into atmosphere with a temperature of 20 °C and a pressure of 100 kPa which stay constant during the simulation.

## 3. Results

There are three parts to the results. First we measure the actuation flow properties with the dual laser beam method (Ju et al., 2010). Second we predict the actuation flow characteristics using our numerical model as described in Ju et al. (2010) with two different multi-component formulations under deep and shallow smoking inhalation profiles for Oxette® 1 and Oxette® 2, and compare the actuation flow velocity, duration and relative density to the experiment results. Finally we predict the residual droplet sizes of the aerosol at $x = 100$ mm with the inputs from the previous analyzed properties of the actuation flow.

### 3.1. Measurements of actuation flow characteristics by the dual laser method

Similar to our previous work (Ju et al., 2010), the data of actuation flow characteristics were recorded by the dual laser beam method at two axial positions of $x = 25$ mm and $x = 100$ mm from the discharge orifice. Please note the results presented below by the dual laser method were recorded from the start of the actuation. Two laser beams form two control volumes across which the spray plume passes. The light intensity change of the two laser beams due to beam obscuration by the spray is detected by two photodiodes and recorded by a PC based data acquisition card (AD). When the spray passes through the first laser beam there will be a drop in voltage waveform from the correlative photodiode and similarly this will occur when it traverses the second beam. The distance between the two laser beams is known (3 mm in this work), and the time delay can be measured by the delayed signal acquired as a result of the spray taking a finite time to traverse the two beams, therefore the spray velocity can be calculated. Here, this time delay is determined by a cross-correlation procedure (Dyakowski and Williams,

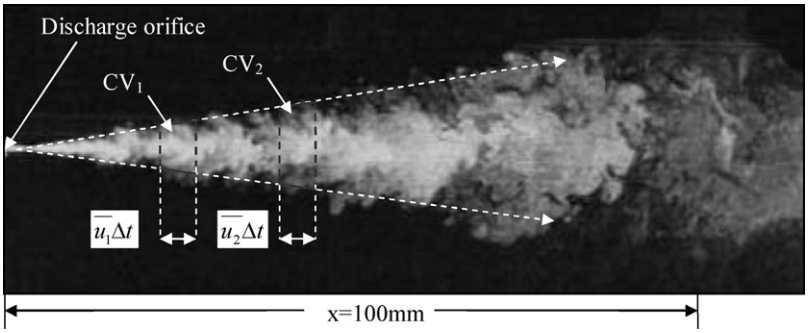


**Fig. 3.** Graphic description about the implementation of the numerical droplet evaporation model to predict droplet sizes at the axial position of $x = 100$ mm from the discharge orifice along a turbulent jet (CV: control volume, $\bar{u}$: local mean velocity, $\Delta t$: time intervals).

1993), which represents the amount of time it takes a spray element to travel through the two laser beams. Furthermore, assuming the spray is uniform and the droplets are spherical, the depth of the voltage drop is proportional to the surface area (of sum of the droplets) occluding the laser beam, and for a given spray mass it is an indication of the droplet sizes. Therefore a non-dimensional relative light obscuration term is introduced, which is defined by the ratio between the voltage drop when the spray transverse though the laser beams and the peak voltage when there is no spray passing. Although this cannot provide the absolute spray concentration or droplet size, it still can provide some relative measurement of spray opacity due to formulation variations.

Oxette® 1 can hardly generate fine sprays with any formulations, and it can only produce large droplets, bulk liquid jets or sheets, which are difficult to be detected by the dual laser beam method. The relative light obscuration for the spray generated by Oxette® 1 during the 1st deep inhalation is shown in Fig. 4, where it shows the relative opacities of the sprays are not comparable to those produced by Oxette® 2 (Fig. 5). Similarly, under the shallow inhalations, it can neither generate fine sprays nor can be detected by the dual beam method.

Fig. 5 shows the relative light obscuration for the spray generated by Oxette® 2 under the 1st deep inhalation. Formulation 1 (95% HFA 134a) generated relatively denser spray than Formulation 2 (98% HFA 134a), which is caused by the lower evaporation rate of Formulation 1 and more non-volatile components remaining. The light obscuration by the spray after inhalation did not return to the original state before the actuation, which is caused by the droplets filled in the inspiration chamber of the mechanical lung. Without an intermediate refill, the spray generated during 2nd deep inhalation was barely detected by the dual laser beam method due to most of the formulation being consumed during the 1st deep inhalation.

Fig. 6 shows relative light obscuration for the spray generated by Oxette® 2 with Formulation 1 (95% HFA 134a) and Formulation 2 (98% HFA 134a) under repeated shallow inhalations without an intermediate refill. The relative density of the sprays decreases at each sequential inhalation and the ratio is 2.8:1.8:1 for Formulation 1 at $x = 25$ mm. Compared to Formulation 1, the mixture vapor pressure of Formulation 2 is higher due to its higher mass fraction of HFA 134a. It actuated more fluid at the exit of the discharge orifice ($x = 25$ mm) and resulted in denser sprays than Formulation 1 at $x = 25$ mm during the first 0.2 s. Again the higher mass fraction of HFA 134a caused a faster evaporation rate, and therefore Formulation 2 produced sparser sprays at $x = 100$ mm compared to Formulation 1.

Several researchers (Yildiz et al., 2002; Calay and Holdo, 2008; Polanco et al., 2010) stated the axial velocity increased during the expansion region and started to decrease in the entrainment region due to mixing with ambient air as jet propagates. The spray expansion region depends upon the geometry of the atomizer, initial conditions of the flow such as superheat level and the liquid properties (Yildiz et al., 2002). More analysis on expansion region characters will be detailed in the accompanying paper (Ju et al., 2012) where the measurements were taken by high speed imaging. Table 1 shows the axial spray velocity calculated by the cross correlation method (Ju et al., 2010) from the dual laser results. At $x = 25$ mm, the jet had higher velocities under the 1st and the 2nd shallow inhalations than that under the 1st deep inhalation. Because under the deep inhalation the jet has shorter expansion region where its velocity starts to decrease earlier than the jet generated under the shallow inhalation. Under sequential shallow inhalations, the axial velocities at $x = 25$ mm decreased due to the consumption of the formulations, however the axial velocities at $x = 100$ mm increased due to the less entrainment occurring.

### 3.2. Prediction of flow characteristics by the numerical multi-component actuation flow model

The actuation flows issuing from the Oxette® were simulated by the previous multi-component actuation flow model (Ju et al., 2010). The flow characteristics at the exit of the discharge orifice, such as axial velocity, gas/liquid mass ratio and liquid temperature, are treated as the initial conditions to predict the initial MMD of the spray at the exit by Eq. (1).

The initial temperatures in the metering chamber and expansion chamber are the same as the conditions for each inhalation: 293 K (20 °C); the pressure in the metering chamber is the mixture vapor pressure at saturated condition and atmospheric temperature. There is air residing in the expansion chamber initially, so the pressure there is atmospheric before each inhalation. The mass flow in the early prototype Oxettes® can only be triggered under the pressure below 96% of the atmospheric pressure. The metering chamber temperature stays the same as the atmospheric temperature at the beginning of each inhalation regardless of how many repeated puffs have been tested.

Temporal variations of the actuation flow properties at the exit of the discharge orifice for the Formulation 1 and Formulation 2

**Table 1**
Axial spray velocity generated by Formulation 1 (95% HFA 134a) and Formulation 2 (98% HFA 134a) with Oxette® 1 under different inhalation profiles at $x = 25$ mm and $x = 100$ mm.

| | Axial spray velocity (m/s) | | | |
|---|---|---|---|---|
| | Formulation 1 | | Formulation 2 | |
| | $x = 25$ mm | $x = 100$ mm | $x = 25$ mm | $x = 100$ mm |
| 1st deep inhalation | 9.38 | 4.17 | 10.71 | 5.36 |
| 1st shallow inhalation | 14.29 | 4.54 | 16.00 | 4.55 |
| 2nd shallow inhalation | 13.64 | 4.55 | 12.00 | 4.62 |
| 3rd shallow inhalation | 13.63 | 6.12 | 9.68 | 6.52 |

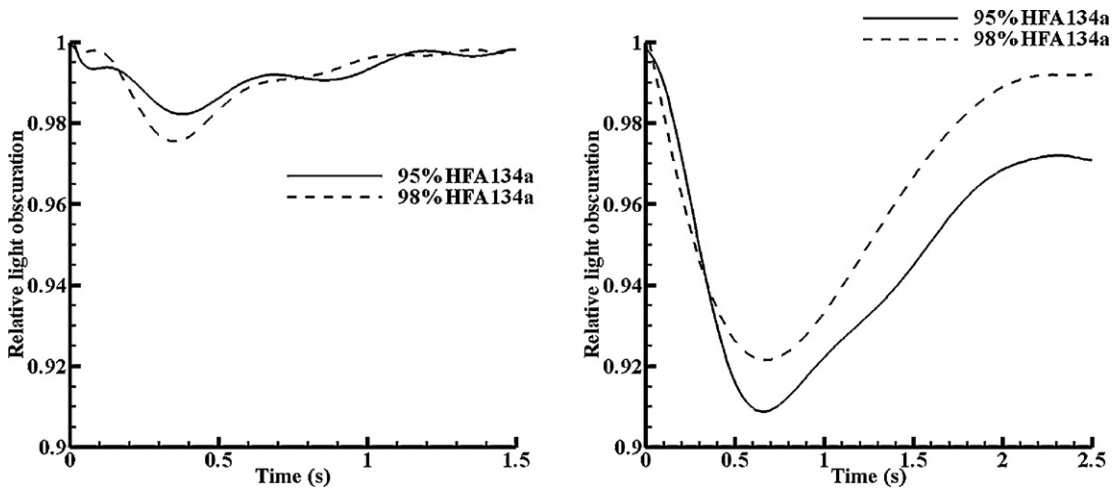


**Fig. 4.** Relative light obscuration for the spray generated by Oxette® 1 with Formulation 1 (95% HFA 134a) and Formulation 2 (98% HFA 134a) under the 1st deep inhalation (due to large droplets, bulk liquid jets or sheets generated near discharge orifice, the relative light obscuration at $x = 25$ mm (left) is much less than that at $x = 100$ mm (right)).

under repeated deep inhalations without an intermediate refill are shown in Fig. 7. Different from the dual laser method, the data was recorded from the start of each smoking profile (Fig. 2). Before the pressure reached below 96% of the atmospheric pressure, the data stayed the same as the initial conditions as shown in Fig. 7 during the first 0.2 s. Oxette® 2 produced a spray with lower mass flow rate (less than 0.17 g/s) than Oxette® 1 (more than 0.22 g/s), because Oxette® 2 has a larger expansion chamber volume and it provides more room to generate small bubbles in the expansion chamber (Sher et al., 2008) and it increases the vapor/liquid mass ratio in the expansion chamber and results in the reduction of the mass flow rate. There are no significant differences between properties of the flows generated by two formulations. Compared to Formulation 1, higher mass flow rates (the peak is 0.168 g/s) generated by Formulation 2 are caused by the higher vapor pressure of the mixture since it contains a higher mass fraction of HFA 134a (98%). For the devices tested only 13.5–17.5% of the formulation is left after the first deep inhalation, which only allows the devices to provide one rich puff under deep inhalation, hence the sprays generated under the 1st and 2nd deep inhalation are very different.

As there is little difference between the actuation flows of the two formulations under sequential time of the shallow inhalation, only for Formulation 1, temporal variations of the actuation flow properties at the exit of the discharge orifice are presented in Fig. 8. The pressure reached 96% of the atmospheric pressure after 0.62 s from the start of shallow inhalation. Compared to the deep inhalation, a similar conclusion can be made. Oxette® 2 generates the flow with lower mass flow rate but higher axial velocity than Oxette® 1, which is due to the larger expansion chamber volume of Oxette® 2. The actuated amount of the formulations decreased after each sequential inhalation, where the spray density ratio, calculated from the predictions of the mass flow rates, at each sequential inhalation is 2.07:1.44:1. The ratio is lower than the measurement by the dual lasers (2.8:1.8:1), because the numerical model predicts the flow at discharge orifice, while the dual laser method measures the spray "accumulated" at $x = 25$ mm where droplets deposit and are pushed forward by the upstream jet. The axial velocities at $x = 25$ mm (the peak is 17 m/s) were larger than the measurement by the dual laser method, especially under the 1st deep inhalation. There is a 40% deviation from the experimental results. It is thought to be caused by the sharp pressure change at the first 0.2 s of the inhalation where turbulent fluctuations influence the velocity measurement by the dual laser method.

The flow model predicted the mass fraction of the formulations actuated during each sequential deep or shallow inhalation as listed in Table 2. More than twice of the formulation was consumed

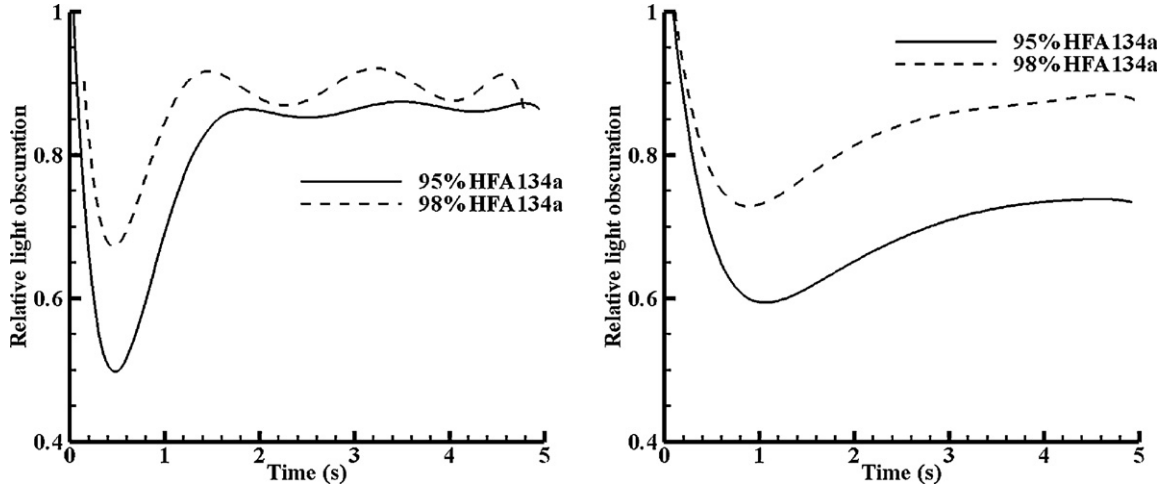


**Fig. 5.** Relative light obscuration (from the dual laser measurement) for the spray generated by Oxette® 2 with Formulation 1 (95% HFA 134a) and Formulation 2 (98% HFA 134a) under the 1st deep inhalation (left: at $x = 25$ mm; right: at $x = 100$ mm).

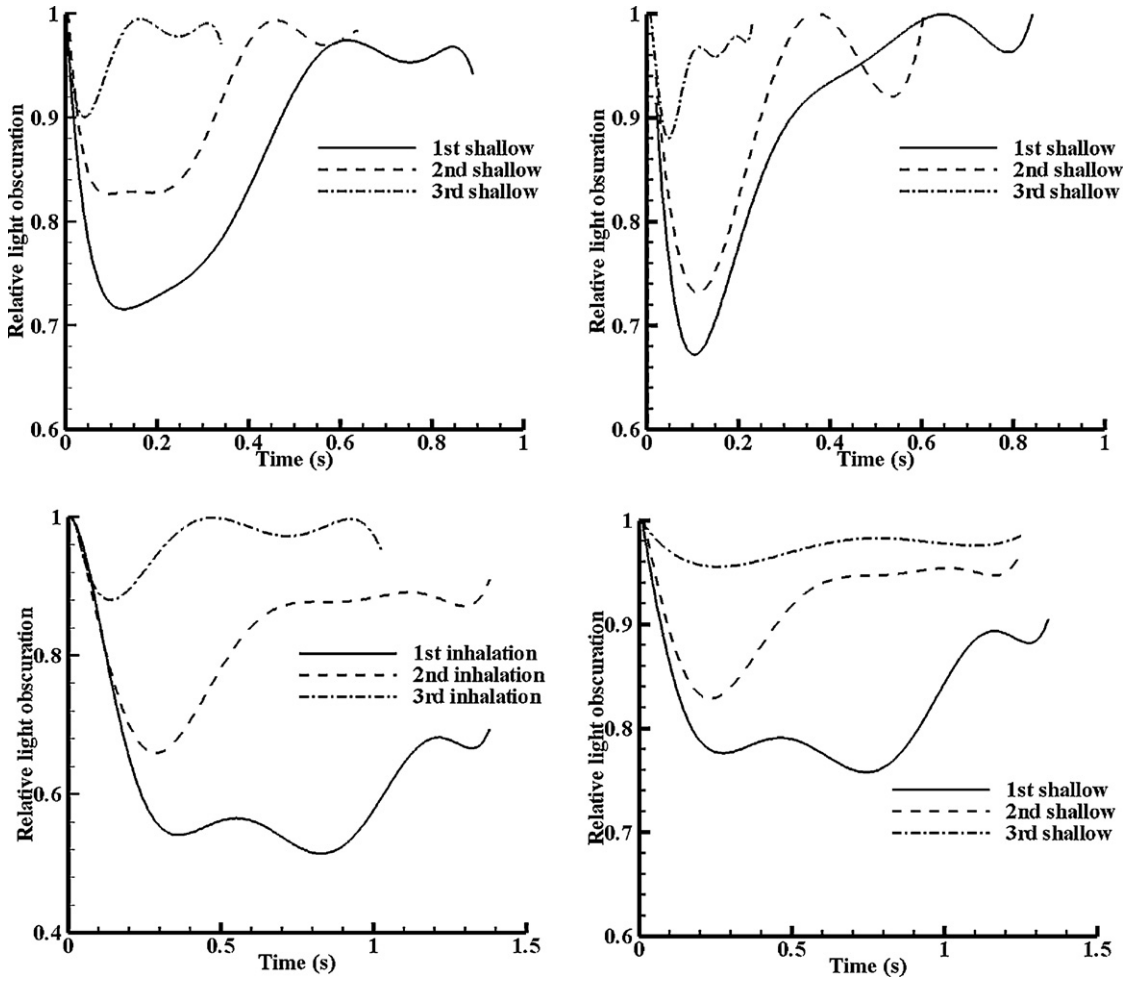


**Fig. 6.** Relative light obscuration (from the dual laser measurement) for the spray generated by Oxette® 2 with Formulation 1 (left column: 95% HFA 134a) and Formulation 2 (right column: 98% HFA 134a) under the 1st, the 2nd and the 3rd shallow inhalation (top row: at $x$ = 25 mm; bottom row: at $x$ = 100 mm).

during the 1st deep inhalation (around 86.0%) than that during the 1st shallow inhalation (around 41.5%). Although mass flow per inhalation is not particularly constant, the results do highlight how the system can react as would a normal cigarette to a deep or a shallow inhalation. Formulation 1 generates steadier and relatively slower actuation flow with Oxette® 2 than with Oxette® 1.

Fig. 9 shows the predictions of initial MMD variations of the sprays at the exit of the discharge orifice for the two formulations under two smoking inhalations, and it illustrates that Formulation 2 produces a spray with slightly smaller droplets than Formulation 2. It indicates that the mass fraction of propellant does not affect the initial MMD very much between these two formulations; hence

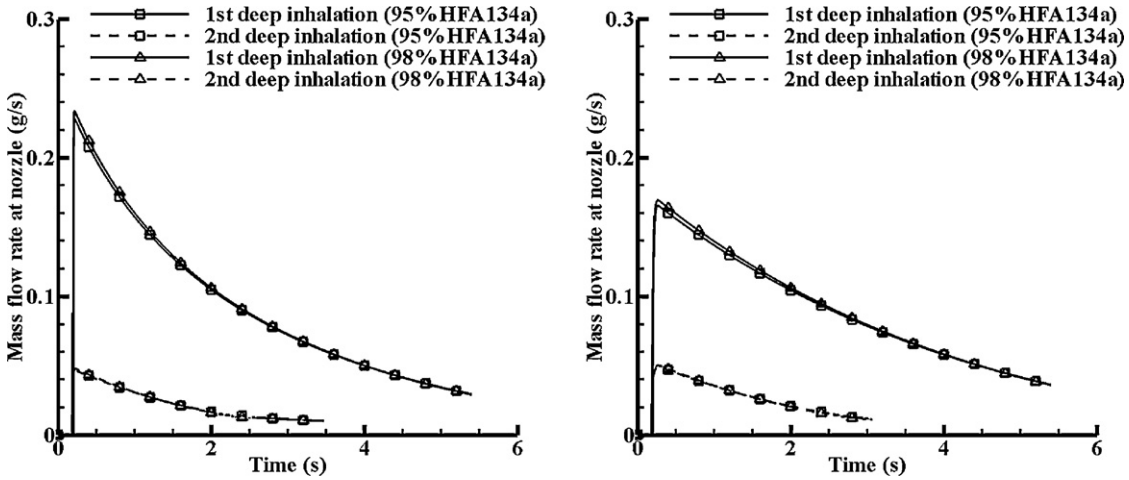


**Fig. 7.** Under sequential times of the deep inhalation, temporal variations of mass flow rates are plotted at the exit of the discharge orifice for two formulations (Formulation 1 with 95% HFA 134a and Formulation 2 with 98% HFA 134a) (Left: Oxette® 1; Right: Oxette® 2).

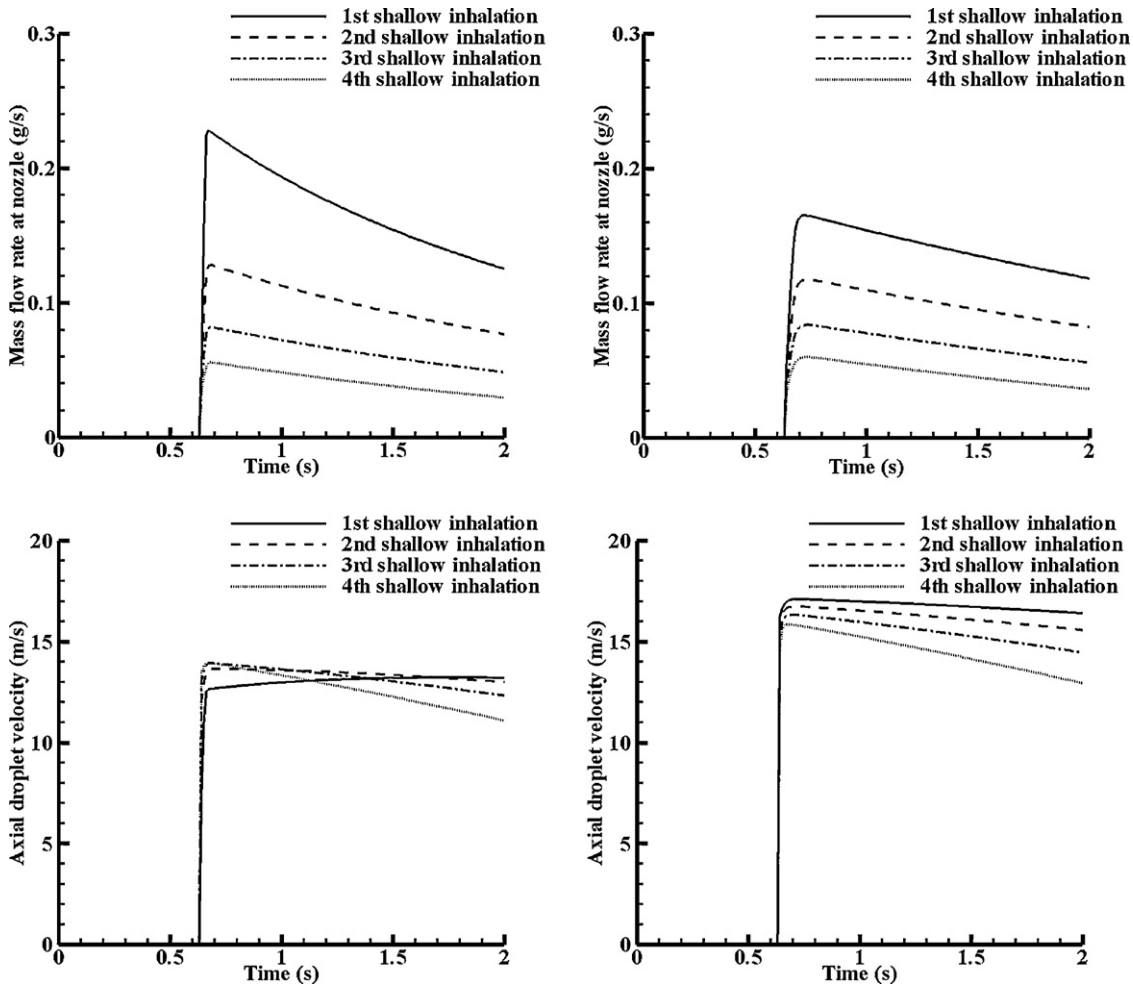


**Fig. 8.** Under sequential times of the shallow inhalation, temporal variations of the actuation flow properties are illustrated at the exit of the discharge orifice for Formulation 1 (95%HFA 134a) (left column: Oxette® 1; right column: Oxette® 2).

we will not present the predicted initial MMD variations of Formulation 2 under the shallow inhalations. Oxette® 1 produces much larger droplet (MMD > 50 μm) during the actuation and does not meet the design requirement. Oxette® 2 performs better; however, larger droplets are generated at the beginning of 1st deep inhalation and 1st shallow inhalation. It is caused by the smaller vapor mass fraction in the expansion chamber, which provides less volume for the propellant evaporation, recirculation, bubble generations and growth to produce small droplets. For the spray produced by Oxette® 2, under 1st deep inhalation, the predicted initial MMD reaches a minimum of 20 μm at 3.5 s. Under 1st shallow inhalation, the predicted initial MMD increases at the start of actuation to the maximum of 36 μm and then decrease to 30 μm at the end of the actuation. The average predicted initial MMD deceases after each shallow inhalation and during the 3rd inhalation it generates the most uniform droplets. Clark (1991) measured the initial MMD of the spray produced by a pMDI as 12.5–22. 5 μm for a formulation with 98% mass fraction of HFA 134a and 2% PEG300 and similarly Dunbar (1996) measured the initial MMD of the spray issued from a pMDI as 7.3 μm with pure HFA 134a. Their measured initial MMDs are smaller than our predictions, because the pMDI has a large expansion chamber of 17.6 $mm^3$, compared to the 5.41 $mm^3$ expansion chamber volume of Oxette® 2, and it provides more space for the bubble formation. Encouraging the bubble formation in the expansion chamber results in the increase of $q_{ec}$ in Eq. (1) and reduces the MMD value.

Large variations of the predicted initial MMD for each sequential (deep and shallow) inhalation are caused by the increase of the quality of fluid ($q_{ec}$) in the expansion chamber (Eq. (1)). Since the mass fraction of the original fill left at the start of the 2nd deep inhalation or the 4th shallow inhalation is less than 13%, fine sprays will not be generated and a refill is required. It should be noted that

**Table 2**
Mass fraction of the formulations actuated during each sequentially deep or shallow inhalation for the Formulation 1 (95%HFA 134a) and Formulation 2 (98% HFA 134a) with Oxette® 1 and Oxette® 2.

| | Deep inhalation | | Shallow inhalation | | | |
|---|---|---|---|---|---|---|
| | 1st | 2nd | 1st | 2nd | 3rd | 4th |
| Formulation 1 (Oxette® 1) | 85.88% | 11.25% | 41.49% | 24.09% | 15.27% | 9.76% |
| Formulation 2 (Oxette® 1) | 86.16% | 11.02% | 41.90% | 24.20% | 15.28% | 9.72% |
| Formulation 1 (Oxette® 2) | 82.85% | 13.18% | 34.77% | 24.13% | 16.80% | 11.40% |
| Formulation 2 (Oxette® 2) | 83.25% | 12.88% | 35.20% | 24.30% | 16.83% | 11.36% |

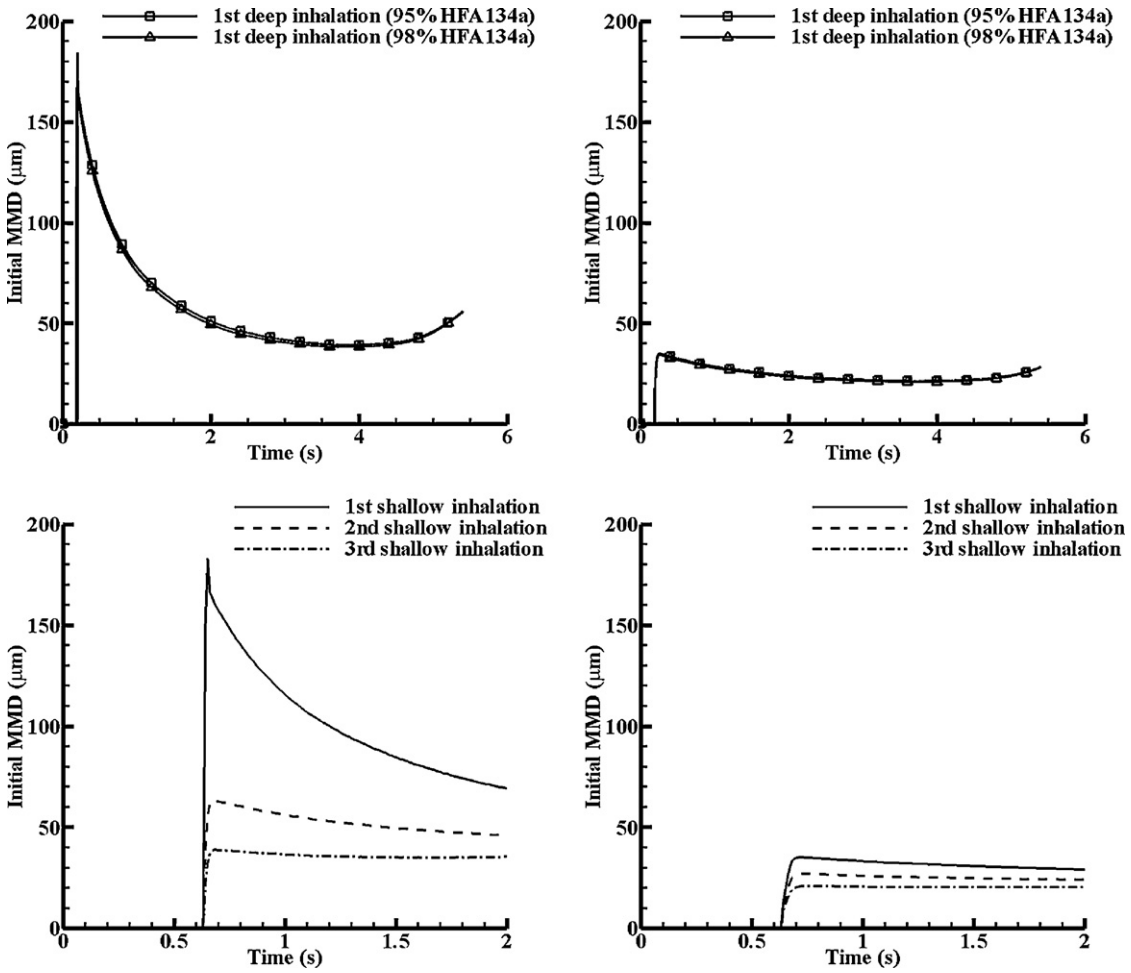


**Fig. 9.** Temporal variations of the predicted initial MMD at the exit of the discharge orifice for Formulation 1 (95%HFA 134a) and Formulation 2 (98%HFA 134a) under the 1st deep inhalation; and only for Formulation 1 under sequential times of the shallow inhalation (left column: Oxette® 1; right column: Oxette® 2).

the qualitative predictions of the model for Oxette® 1 and Oxette® 2 are in agreement with the experiment in that the obscuration is much less for Oxette® 1 and that the model predicts far larger primary drops. On the other hand the effect of the formulation is much more sensitive in reality than is predicted in the model. This can be due to the simple equilibrium evaporation assumption that is assumed in the model. The model does however show more variation for Oxette® 1 compared to Oxette® 2.

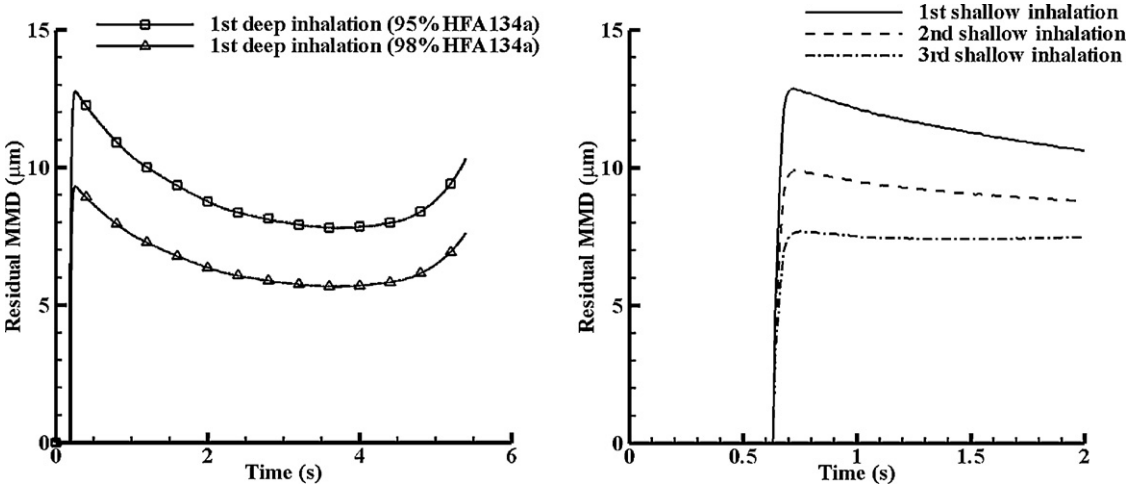


**Fig. 10.** Temporal variations of predicted residual MMDs of the spray generated by Oxette® 2 at $x = 100$ mm from the discharge orifice for Formulation 1 (95%HFA 134a) and Formulation 2 (98%HFA 134a) under the 1st deep inhalation (left); and only for Formulation 1 under sequential shallow inhalations (right). The effect of the mass fraction of HFA 134a is more obvious here than that in Fig. 9.

### 3.3. Prediction of residual droplet sizes of the aerosol at $x = 100$ mm from the discharge orifice

With the known velocities, temperatures and vapor/liquid mass ratios of the actuation flow which were analyzed previously, the residual droplet sizes of the spray at $x = 100$ mm from the discharge orifice can be predicted from the initial droplet sizes at the exit of the discharge orifice due to the evaporation of the droplet, following the assumptions of the multi-component evaporation model of Brenn et al. (2007) in Section 2.2. The axial velocities of the droplets are assumed to vary linearly along the jet from the exit of the discharge orifice to $x = 100$ mm (Calay and Holdo, 2008; Polanco et al., 2010), with the boundary conditions of the flow velocities at $x = 100$ mm measured by the dual laser method (Table 1).

Following the predicted initial MMDs at the exit of the discharge orifice acquired previously (Fig. 9), the residual MMDs at $x = 100$ mm predicted by the multi-component evaporation model (Brenn et al., 2007) are shown in Fig. 10. As stated previously, the mass fraction of the propellant (for the two formulations) does not affect the predicted initial MMD at the exit of the discharge orifice under the 1st deep inhalation (Fig. 9); it does however influence the predicted residual MMD at $x = 100$ mm under the 1st deep inhalation (Fig. 10). With higher mass fraction of HFA 134a, Formulation 2 produced smaller droplets than Formulation 1. The ratio of the predicted residual MMDs of the droplets generated by Formulation 2 and Formulation 1 is 0.73, which is the same as the 1/3 order of the ratio of the mass fraction of the inerts (non-volatile components) between two formulations. At $x = 100$ mm, the residual MMD of the spray issued from a pMDI measured by Dunbar (1996) is 6.1 μm with pure HFA 134a, which is smaller than our predictions. The difference is caused not only by the smaller expansion chamber volume of the Oxette®, but also because the mass fraction of inerts in our formulations is larger than that in the case of Dunbar (1996).

## 4. Conclusion

A prediction of residual MMD of the spray issuing from pMDI devices has been added to the previous numerical model (Ju et al., 2010) to understand how operational variables affect the spray's quality, using an evaporation model of multi-component liquid droplets. Two different formulations with 95% and 98% mass fraction of HFA 134a and two early stage prototype cigarette designs with different expansion chamber volumes have been analyzed by the numerical model, with comparisons with the dual laser measurements. Although Formulation 2 can generate smaller droplets, Formulation 1 produces more steady puffs with relatively low mass flow rate. It is concluded that the larger the expansion chamber volume, the more residual room for the propellant evaporation, recirculation, bubble generations and growth, and better sprays are generated. Compared to the earlier design (Oxette® 1), the later design (Oxette® 2) made a significant improvement to produce fine sprays and facilitated development of the cigarette alternative.

## Acknowledgments

We appreciated the technical support from Simon.R.Klitz and funding and prototypes supplement from Kind Consumer Ltd. (http://www.kindconsumer.com/).

## References

Brenn, G., Deviprasath, L.J., Durst, F., Fink, C., 2007. Evaporation of acoustically levitated multi-component liquid droplets. Int. J. Heat Mass Transfer 50 (25–26), 5073–5086.
Calay, R.K., Holdo, A.E., 2008. Modeling the dispersion of flashing jets using CFD. J. Hazard. Mater. 154, 1198–1209.
Clark, A.R., 1991. Metered atomization for respiratory drug delivery. Ph.D. Thesis, Loughborough University of Technology, UK.
Dunbar, C.A., 1996. An experimental and the theoretical investigation of the spray issued from a pressurized metered-dose inhaler, Ph.D. Thesis, Institute of Science and Technology, University of Manchester, UK.
Dyakowski, T., Williams, R.A., 1993. Measurement of particle velocity distribution in a vertical channel. Powder Technol. 77, 135–142.
Fukuchi, K., Miyoshi, K., Watanabe, T., Yonezawa, S., Arai, Y., 2001. Measurement and correlation of infinite dilution activity coefficients of bis(2,2,2-trifluoroethyl)ether in dodecane or alkanol. Fluid Phase Equilib. 182, 257–263.
Gebauer, C.L., 1901. Receptacle for containing and administering volatile liquids. U.S. Patent Publication No. 668,815.
Gebauer, C.L., 1902. Receptacle for containing and administering volatile liquids. U.S. Patent Publication No. 711,045.
Hou, S., Duan, Y., Wang, X., 2008. Vapor–liquid equilibria predictions for alternative working fluids at low and moderate pressures. Ind. Eng. Chem. Res. 47, 7501–7508.
Ju, D., Shrimpton, J., Hearn, A., 2010. The effect of reduction of propellant mass fraction on the injection profile of metered dose inhalers. Int. J. Pharm. 391, 221–229.
Ju, D., Shrimpton, J., Hearn, A., 2012. Effect of expansion chamber geometry on atomization and spray dispersion characters of a flashing mixture containing inerts. Part II. High speed imaging measurements. Int. J. Pharm.
Katz-Zeigerson, M., Sher, E., 1998. Spray formation by flashing of a binary mixture: a parametric study. Atomization Sprays 8, 255–266.
Medicines Healthcare products Regulatory Agency (MHRA), 2010. The Regulation Of Nicotine Containing Products, Consultation Document MLX 364.
Placke, M.E., Ding, J., Zimlich Jr., W.C., 2006–2007. Inhalation: liquids. In: Swarbrick, J. (Ed.), Encyclopedia of Pharmaceutical Technology, vol. 3. , 3rd ed. Informa Healthcare Inc., USA, New York.
Polanco, G., Holdo, A.E., Munday, G., 2010. General review of flashing jet studies. J. Hazard. Mater. 173, 2–18.
Pope, S.B., 2000. Turbulent Flows. Cambridge University Press, Cambridge, UK.
Rashkovan, A., Sher, E., 2006. Flow pattern observations of gasoline dissolved $CO_2$ inside an injector. Atomization Sprays 16, 615–626.
Reid, R.C., Prausnitz, J.M., Sherwood, T.K., 1977. The Properties of Gases and Liquids, 3rd ed. McGraw-Hill, New York, USA.
Sanders, P.A., 1970. Principles of Aerosol Technology. Van Nostrand Reinhold Co, New York, USA.
Scollo, M., Lal, A., Hyland, A., Glantz, S., 2003. Review of the quality of studies on the economic effects of smoke-free policies on the hospitality industry. Tobacco Control 12, 13–20.
Sher, E., Bar-Kohany, T., Rashkovan, A., 2008. Flash-boiling atomization. Prog. Energy Combust. Sci. 34, 417–439.
Tobin, M.J., Jenouri, G., Sackner, M.A., 1982. Subjective and objective measurement of cigarette smoke inhalation. Chest 82, 696–700.
Wittig, R., Lohmann, J., Gmehling, J., 2003. Vapor–liquid equilibria by UNIFAC Group Contribution. 6. Revision and Extension. Ind. Eng. Chem. Res. 42, 183–188.
Yildiz, D., Rambaud, P., Vanbeeck, J., Buchlin, J.M., 2002. A Study on the Dynamics of a Flashing Jet. Final Contract Research Report EAR0030/2002. von Karman Institute for Fluid Dynamics.